Description of Supplementary Files

File Name: Supplementary Information

Description: Supplementary figures

File Name: Peer Review File

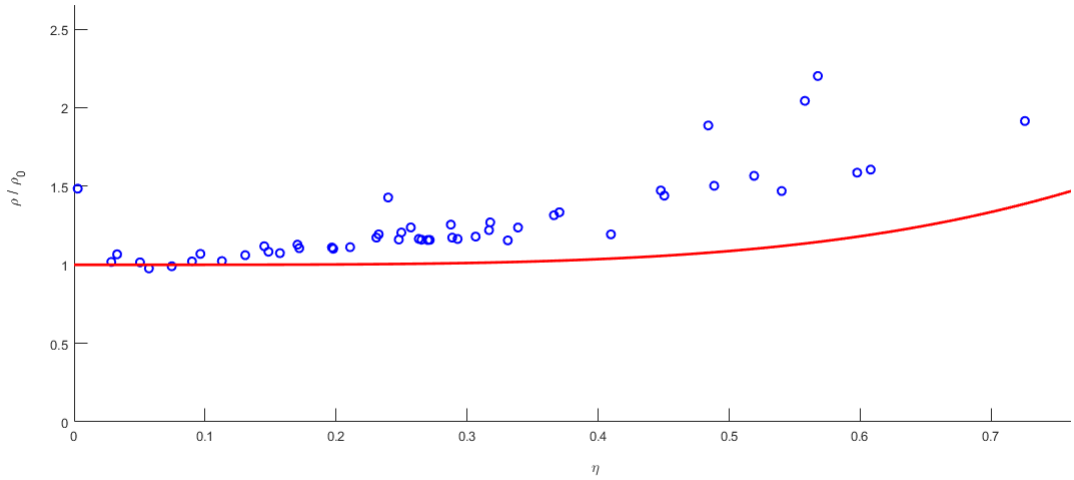

Supplementary Figure 1. Dronpa-DAT forms clusters in the plasma membrane of CAD cells as demonstrated by an analysis method from Baumgart et al. (**a**) The normalized average density of localization present in clusters (ρ/ρ_0) was compared to the relative area of the ROI covered by a cluster mask (η), with each data point being a 5 µm by 5 µm ROI from a CAD cell expressing Dronpa-DAT and imaged with PALM. The red line indicates a reference curve from a random distribution.

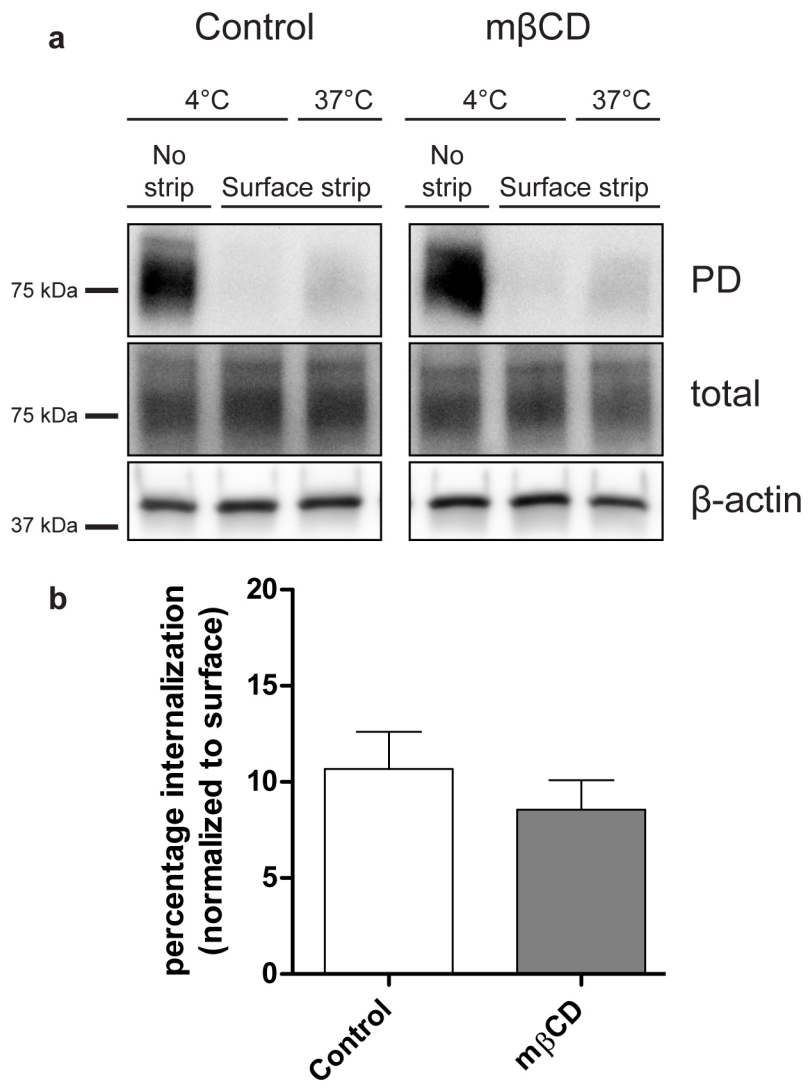

Supplementary Figure 2. Cholesterol depletion does not affect DAT internalization in CAD cells. Reversible biotinylation assay on CAD cells assessing the internalization of DAT over 30 min at 37°C without or with cholesterol depletion with mβCD (**a**) *Top panels*; western blotting for biotinylated, pulled-down DAT (PD) (control, mβCD). Lanes 1 and 2 from left (4 °C) show total surface immunosignal (no stripping with MesNa) and after stripping (+MesNa). Lane 3 shows internalized DAT (37 °C). Middle panels, western blotting for total DAT; Lower panels; western blotting for actin. (**b**) Quantifications of internalized DAT minus the stripping control as a percentage of total surface DAT (mean ± s.e.m. not significant according to a an unpaired, two-tailed t-test, control: n = 4, mβCD: n = 5.

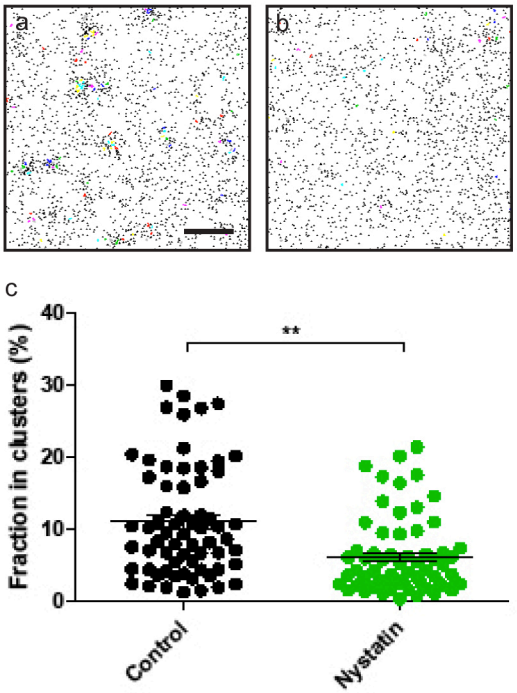

Supplementary Figure 3. Cholesterol sequestration by nystatin decreases DAT clustering in CAD cells. CAD cells transiently expressing Dronpa-DAT were treated for 20 min treatment at 37°C with vehicle or 10 µg ml^{-1} nystatin prior to PALM imaging. (**a, b**) DBSCAN-based cluster maps of Dronpa-DAT distribution in CAD cells without (**a**) or with nystatin (**b**). Clustered localizations are shown by color-coding with non-clustered localizations in grey. (**c**) Clustering of Dronpa-DAT given as the fraction of localizations in clusters in % (mean ± s.e.m.,**p<0.01, unpaired, two-tailed t-test). Data are based on 129 cells from 3 independent experiments. Scale bar 1 µm

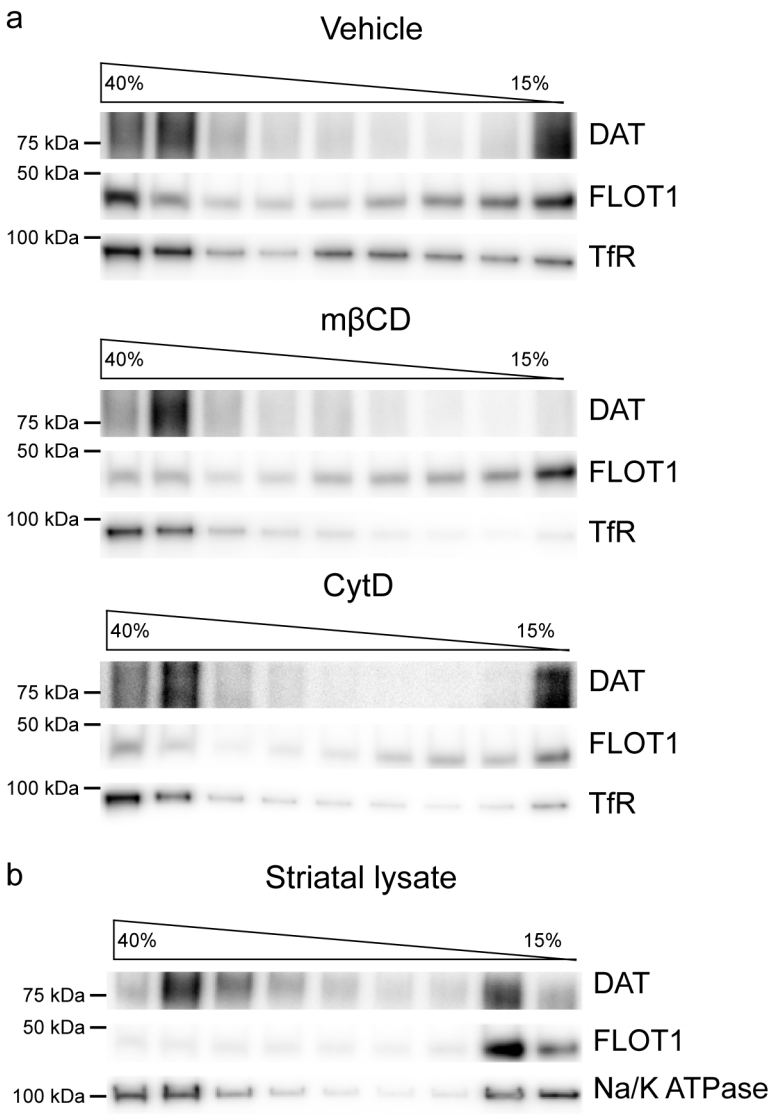

Supplementary Figure 4. DAT segregates into detergent-resistant low buoyancy membrane fractions in a cholesterol-dependent manner. (**a**,**b**) Sucrose-based density gradient fractionation of DAT in lysates of CAD cells and mouse striatum. Cells or mice striatal tissue were lysed using 1% Brij58 and mixed with 80% sucrose in a continuous sucrose gradient from 40-15%. Subsequently the sucrose gradient was centrifugated for 18 h at 100,000 x g and divided into ten fractions. The fractions were analyzed by western blotting using specific antibodies for indicated proteins. (**a**) Vehicle treated cells transiently expressing the transferrin receptor (TfR) and DAT. DAT segregates both into high-buoyancy fractions together with TfR and into low-buoyancy fractions together with the (endogenous) membrane-raft marker, flotillin-1 (FLOT1). Cholesterol depletion with 5 mM methyl-β-cyclodextrin (mβCD) but not actin depolymerization with 5 μg ml^{-1} cytochalasin D (CytD) disrupted segregation of DAT into low-buoyancy fraction. Representative cropped western blots for entire membranes developed for horseradish peroxidase, see Supplementary Figure 8. (**b**) Endogenous DAT also segregates into both high-buoyancy fractions together with the Na^+/K^+ ATPase and into low-buoyancy fractions together with flotillin-1 (FLOT1). Immunoblots shown are representative of three experiments with similar results.

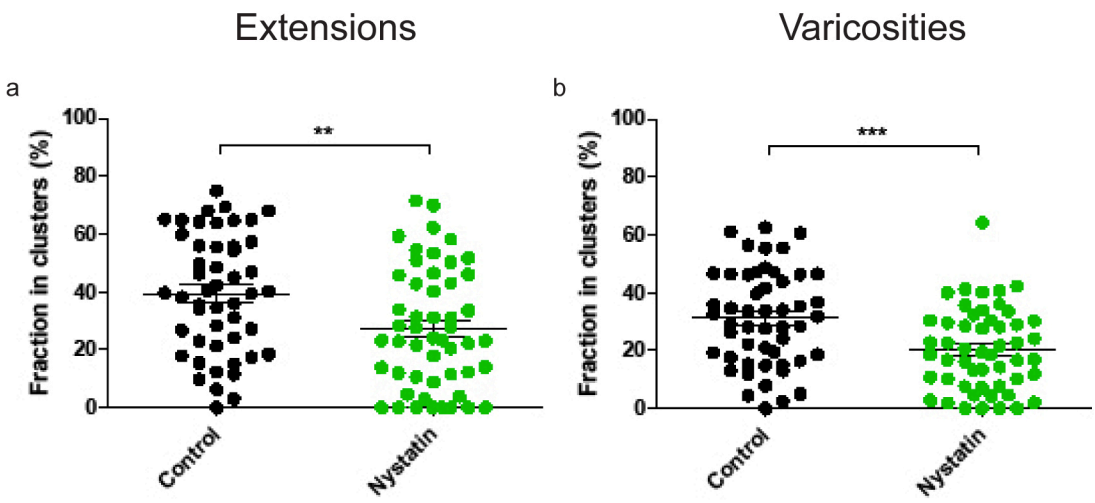

Supplementary Figure 5. Cholesterol sequestration by nystatin decreases DAT clustering in dopaminergic neurons. Cultered dopaminergic were treated for 20 min at 37°C with vehicle or 10 µg ml^{-1} nystatin prior to fixation and staining for DAT using anti-DAT antibody and Alexa405-Alexa647-conjugated secondary antibody. The resulting STORM images were analyzed by DBSCAN. (**a, b**) Clustering of endogenous DAT as assessed by DBSCAN in neuronal extensions and varicosities given as the fraction of localizations in clusters in % (means ± s.e.m., **p<0.01, ***p<0.001, unpaired, two-tailed t-test). Data are based on 99 cells from 3 independent experiments.

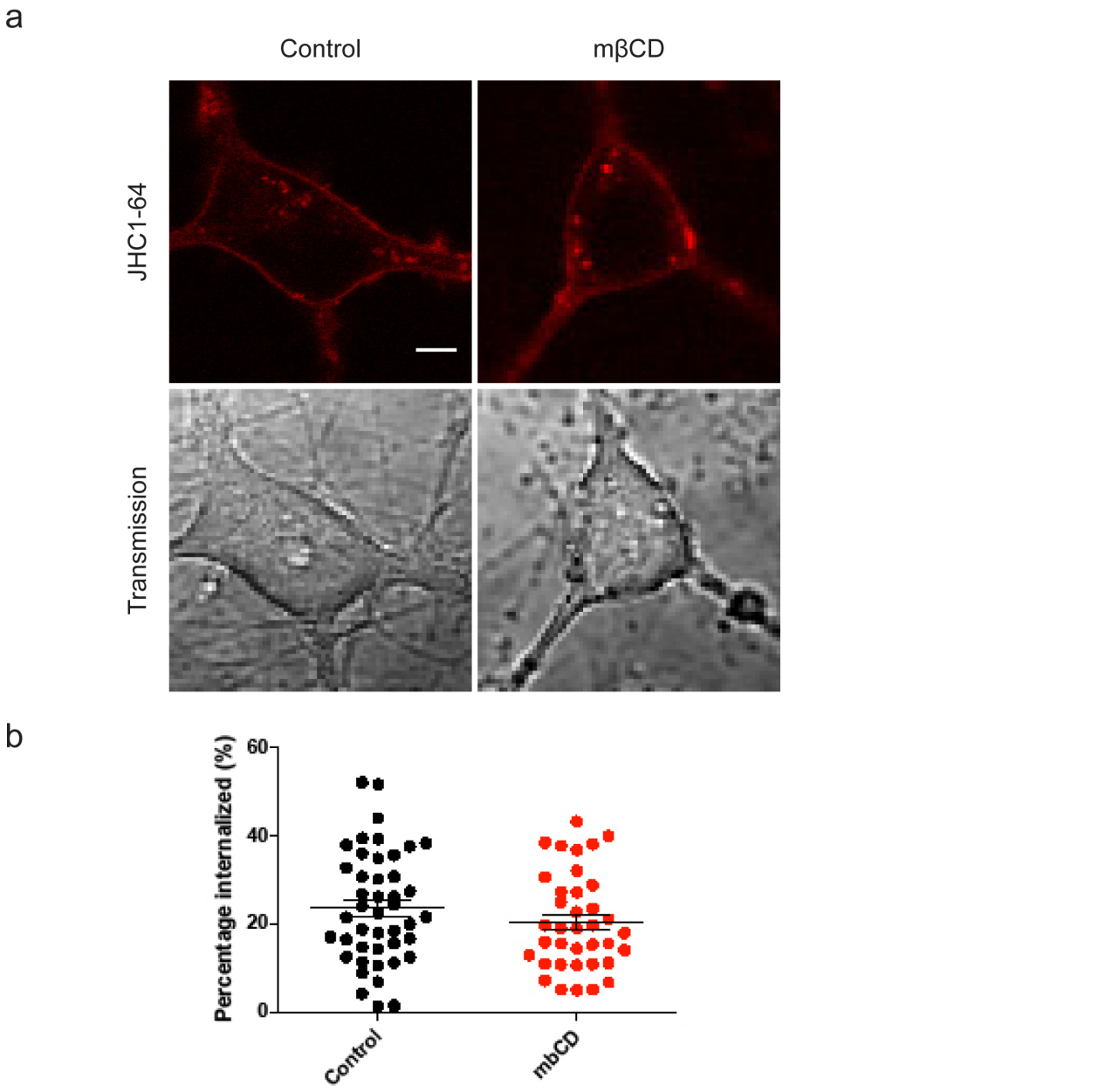

Supplementary Figure 6. Cholesterol removal does not influence the internalization DAT in cultured dopaminergic neurons. (**a**) *Top panel,* Confocal images of representative live dopaminergic neurons showing internalization of DAT labeled with the fluorescent cocaine-analogue JHC 1-64. The neurons were labeled for 20 min with 20 nM JHC1-64 at 4°C before incubation for 30 min at 37°C with vehicle (control) or 5 mM m β CD followed by further 30 min incubation at 37°C. *Bottom panel*, transmission images of the cells shown in the *Top panel*. (**b**) Quantification of internalized JHC 1-64 – labeled DAT after 1 h at 37°C expressed as the fraction of intracellular JHC1-64 signal relative to the cell surface (Mean±s.e.m.; not significant according to an unpaired, two-tailed t-test). Data are based on 37-44 cells from 3 independent experiments. Scale bar 500 nm.

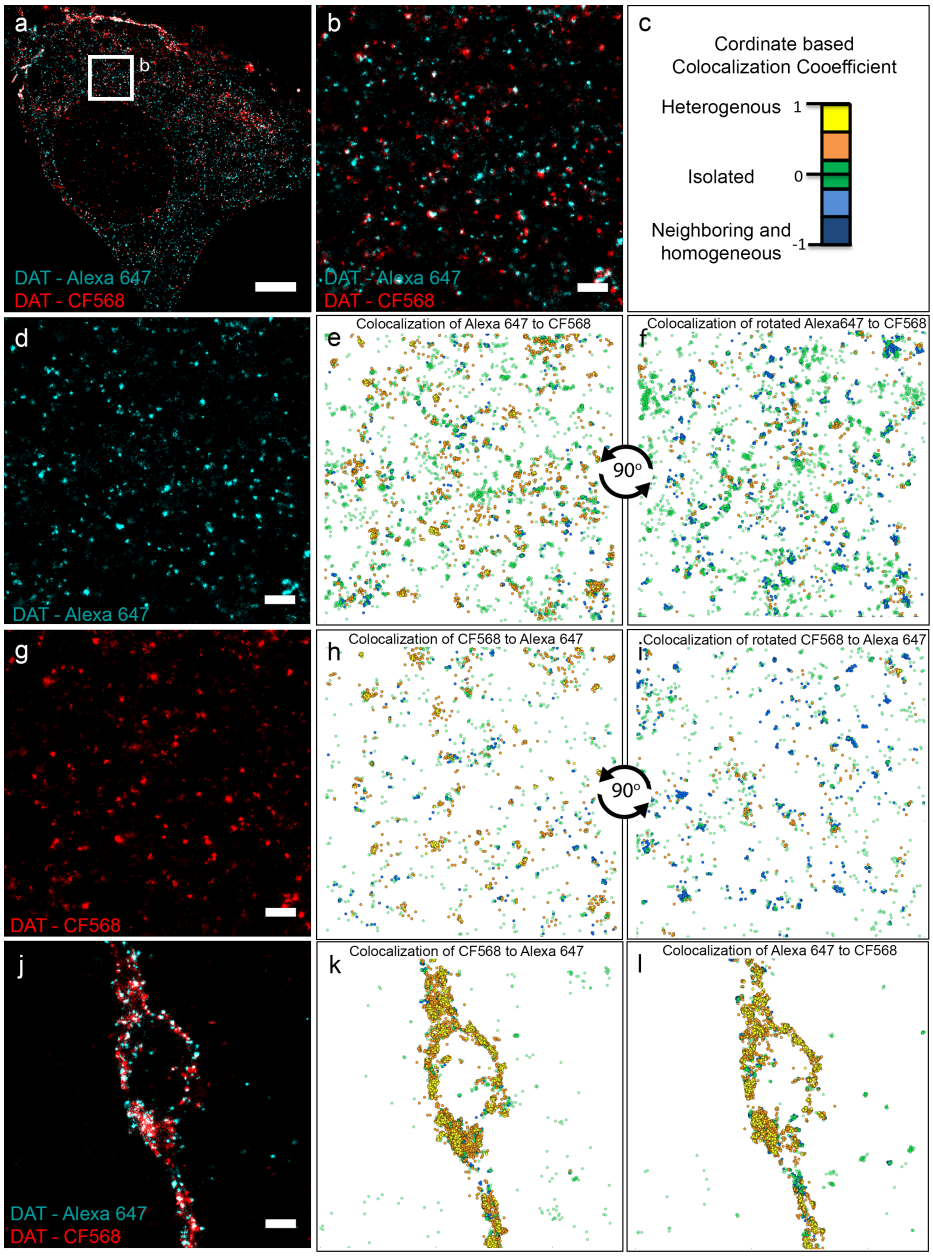

Supplementary Figure 7. Dual-color dSTORM images of DAT, colabeled with two spectrally separate fluorophore-conjugated secondary antibodies, identify similar protein distributions on dopaminergic neurons. (**a**) Cross-section views through the cell body of a dopaminergic neuron showing the distribution of DAT with the two spectrally separate labels by dSTORM imaging. (**b**) Enlarged view of the dSTORM image corresponding to the boxed region in **a**. (**c**) Color code for colocalization identification used in images **e,f,h,i**. (**d**) Localizations detected from Alexa 647 in image **b**. (**e**) Colocalization of Alexa647 localizations to CF568 localizations. (**f**) Colocalization of Alexa647 localizations after a 90^0 rotation to CF568 localizations. (**g**) Localizations detected from CF568 in image **b**. (**h**) Colocalization of CF568 localizations to Alexa647 localizations. (**i**) Colocalization of CF568 localizations after a 90^0 rotation to Alexa647 localizations. (**j**) Dual-color dSTORM image for DAT on a varicosity of a dopaminergic neuronal process. (**k**) Colocalization of CF568 localizations to Alexa647 localizations from image **j**. (**l**) Colocalization of Alexa647 localizations to CF568 localizations from image **j**. Scale bars **a** 4 µm, **b,d,g,j** 0.5 µm.

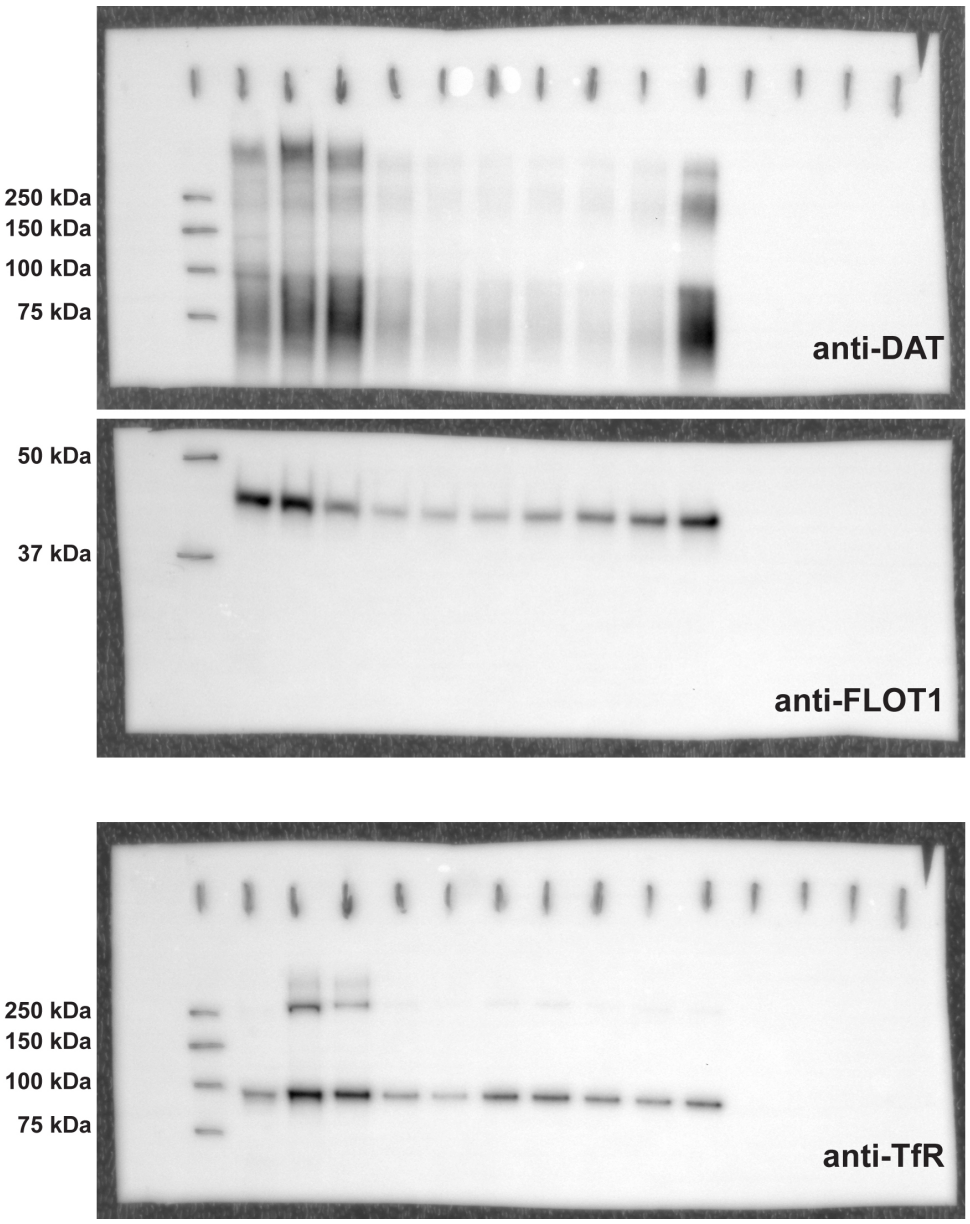

Supplementary Figure 8. Scan of uncropped western blot membranes of sucrose gradients samples developed for horseradish peroxidase. Sucrose gradient samples were loaded to an 'any KD', precast gel and transferred on to a PVDF membrane. The membrane was cut in two and developed for DAT using rat anti-DAT antibody, flotillin-1 (FLOT1) using rabit anti-FLOT1 antibody, and the transferrin receptor (TfR) using mouse anti-TfR antibody. The signal was amplified with HRP-conjugated secondary antibody and developed with ECL prime western blotting reagent.